Materials Advances

ROYAL SOCIETY OF CHEMISTRY

PAPER

View Article Online
View Journal | View Issue

Cite this: *Mater. Adv.*, 2024, 5, 9471

Enabling improved PSF nanocomposite membrane for wastewater treatment with selective nanotubular morphology of PANI/ZnO†

Aqsa Zahid,[a] Hafiza Hifza Nawaz,[b] Amna Siddique,[a] Basheer Ahmed,[a] Shumaila Razzaque,[c] Xuqing Liu,[d] Humaira Razzaq *[a] and Muhammad Umar *[b]

Increased population and rapid industrialization are depleting and polluting the fresh water resources at an alarming rate, leading to freshwater scarcity. Water pollution caused by heavy metal ions and dyes has become a major problem and has numerous adverse effects on human health. In recent years, nanotechnology has gained much attention in the field of water purification but new approaches in nanomaterials are still required to boost their removal efficiency. This study deals with membrane fabrication by using a novel hybrid polysulfone (PSF)/polyaniline (PANI) nanotube with zinc oxide (ZnO) nanorods *via* the phase inversion method. Two different schemes were employed for membrane fabrication, *i.e.* PSF/PANI blend and ZnO–(PSF/PANI). Nanomaterials were characterized by FTIR, UV, SEM and XRD. Membrane properties such as porosity, pure water flux (PWF), contact angles, solvent contents, protein rejection and flux recovery ratio (FRR) were studied. Incorporation of PANI and ZnO as nanofillers significantly improved solvent content, lowered water contact angles and enhanced anti-fouling properties. The FRR reached about 87.4% and PWF also increased from 20 to 136.3 L m^{-2} h^{-1} bar^{-1} representing enhanced hydrophilicity. Among various compositions, the PP 0.25 nanocomposite membrane demonstrated a maximum removal of 91.2% MB and 94.3% Mn^{7+} and PPZ 0.25 showed removal of 95.18% MB and 96.21% Mn^{7+} at 0.1 MPa. Based on the above results, the PSF/PANI and ZnO–(PSF/PANI) nanocomposite membranes are recommended for practical use in wastewater treatment.

Received 28th August 2024,
Accepted 1st November 2024

DOI: 10.1039/d4ma00859f

rsc.li/materials-advances

1. Introduction

Water reuse and innovative wastewater treatment technologies may provide viable solutions to assist in developing resilience against the escalating challenges posed by water scarcity. The wastewater excreted by textile, dyeing, printing, paper manufacturing and leather industries is immensely enriched with ions of heavy metals and organic dyes.[1] These metal ions and organic dyes are poisonous, carcinogenic, and non-biodegradable.[2] The release of untreated wastewater with such qualities into the environment is absolutely prohibited. The use of such hazardous water implies an imminent danger to the entire ecological system. Much of the organic pollutants and heavy metal ions are successfully removed by conventional wastewater treatment methods such as sedimentation, adsorption, and oxidation.[3] Heavy metal ions and residual organic pigments are frequently present in treated water owing to their intricate structure.[4] Therefore, it is crucial to develop strategies that can effectively and simultaneously eliminate these residual organic dyes and heavy metal ions from wastewater. Membrane separation technology[5] has garnered significant interest because it may produce filtered effluent of higher quality, use fewer chemicals, and occupy smaller physical space than traditional techniques.[6]

In general, membrane materials are classified as either organic or inorganic.[7] Polysulfone (PSF) is an organic polymer, renowned for its exceptional thermal stability, robust mechanical properties and chemical resistance.[8] Due to these characteristics,

[a] *Department of Chemistry, University of Wah, Quaid Avenue, Wah 47040, Pakistan. E-mail: uw-21-chm-ms-020@student.uow.edu.pk, uw-20s-chm-phd-002@student.uow.edu.pk, uw-18-chm-ms-005@student.uow.edu.pk, humaira.razzaq@uow.edu.pk*
[b] *Department of Materials, University of Manchester, Oxford Road, Manchester, M13 9PL, UK. E-mail: hafizahifza.nawaz@manchester.ac.uk, muhammad.umar@manchester.ac.uk*
[c] *Institute of Physical Chemistry, Polish Academy of Sciences, Kasprzaka 44/52, 01-224 Warsaw, Poland. E-mail: srazzaque@ichf.edu.pl*
[d] *State Key Laboratory of Solidification Processing, Centre of Advanced Lubrication and Seal Materials, School of Materials Science and Engineering, Northwestern Polytechnical University, Xi'an, Shanxi 710072, China. E-mail: xqliu@nwpu.edu.cn*

† Electronic supplementary information (ESI) available. See DOI: https://doi.org/10.1039/d4ma00859f

the PSF ultrafiltration (UF) membrane is often used as the primary building block for fabricating composite membranes which are implemented in numerous sectors, including reverse osmosis, chemical processing, water treatment and biomedicine.[9] This attractiveness is attributed to its extensive accessibility, cost-effectiveness, uncomplicated manufacturing process, resistance to thermal, chemical and microbiological factors and ability to operate effectively in a broad pH range.[10] Pervasive implementation of these membranes in industrial applications is impeded by their conspicuous fouling issues and limited flux, which are caused by their hydrophobic properties. In addition, the limited porosity and hydrophobic surface of these membranes negatively affect the performance of composite membranes.[11–13]

A variety of strategies have been used to improve the hydrophilicity, fouling resistance, and mechanical robustness of membranes, enabling them to be tailored with desired attributes.[14] These approaches encompass surface coating, artificial graft alteration and physical mixing. Specifically, incorporating mixing modifications is a simple yet effective strategy for large-scale industrial processes.[15] This production method offers an attractive approach for creating ultrafiltration (UF) membranes, impacting both the surface and internal pore structure of the membrane.[12]

A variety of hybrid ultrafiltration (UF) membranes based on PSF have been created by integrating different additives through mixing adjustment for environmental applications.[16] Previously, carbon-based nanofillers were employed to boost the characteristics of membranes.[12,17,18] Nasseri *et al.* created a PSF–ZnO nanocomposite membrane using the phase inversion approach to remove arsenate from water.[19] The maximum arsenate rejection was 83.685% at 4 bar. Ghasemi *et al.* used a ZnO-doped PSF nanocomposite membrane to remove MB dye from water, which resulted in increased hydrophilicity and a greater rejection rate than the original PSF membrane.[20] Sulfonated ZnO was incorporated in a PSF membrane by Kang *et al.*[21] to improve the membrane's hydrophilicity, permeability and antifouling characteristics. Kumar *et al.*[22] created a ZnO–PSF nanocomposite membrane by incorporating TiO_2 nanoparticles. The purpose was to enhance fouling resistance and facilitate the separation of humic acid from water. A nanofiltration PSF membrane was developed by Qi *et al.*[23] using modified polyethyleneimine which increased its positive charge. This improvement increased the membrane's capacity to effectively remove heavy metal ions and dyes.[24]

Polyaniline (PANI) is an organic conductive polymer[25] that possesses notable attributes such as robust environmental durability,[26] remarkable ability to resist metal corrosion,[27,28] cost-effectiveness,[25] and facile synthesis, and therefore, shows considerable potential for an extensive selection of applications in different industry sectors. PANI nanoparticles with amino groups disperse more effectively than inorganic nanomaterials. The hydrophilic modification of polymeric membrane materials is thought to be favorably affected by these groups.[29] Yuan *et al.* devised a PSF membrane through the integration of PANI, a beneficial additive that increased the membrane's transparency and clogging resistance.[30] The PANI/PSF blended membranes (PPMs) showed improved performance compared to natural PSF membranes. The pure water flux increased by 2.4 times, and the tensile strength also increased. Goel *et al.*[31] conducted a study which showed that modifying the surface of the polysulfone (PSF) membrane through solution polymerization of aniline utilizing $FeCl_3$, $CuCl_2$, and APS catalysts enhances its physiochemical characteristics such as permeability, protein rejection and antifouling.[32] The PSF/PANI–$CuCl_2$ membrane has the most favorable performance, characterized by elevated pure water flow and protein solution penetration flux, as well as exceptional resistance to biofouling. A porous nanofibrous membrane was designed by Song *et al.*[33] using a solution-blowing approach and a combination of PSF/*N*,*N*-dimethylacetamide (DMAc) and tetrahydrofuran (THF). The nanofibers were polymerized with polyaniline (PANI) and polydopamine (PDA) to modify their properties. As THF concentration increased, the nanofibers' surface area and pore size increased, and they effectively removed methyl orange and methylene blue dye from wastewater. In water treatment, fouling of membranes is a major concern, and therefore, monitoring techniques are required to prevent membrane damage or replacement. In order to monitor fouling online, conductive composite ultrafiltration membranes comprised of polyaniline nanofibers and MWCNTs were implemented by Yuan *et al.*[34] In addition to increased conductivity and water flux, the blended membranes rejected 94.2% of bovine serum albumin and reduced resistance significantly. Another study demonstrated a method to improve membrane antifouling characteristics by integrating polyaniline (PANI) with TiO_2 particles. These nanoparticles were infused into polysulfone (PSF) to create ultrafiltration nanocomposite membranes, serving as both internal and external additives. Nanocomposite membranes possess greater porosity, diminished macro-voids and enlarged surface holes as compared to conventional PSF membranes. Moreover, a higher nanoparticle concentration resulted in notable particle agglomeration and reduced antifouling characteristics of the nanocomposite membranes. Thus, polymer blending is a preferable approach to enhance the conductivity of PSF membranes and increase their overall performance. To remove both metal ions and dyes at the same time, the PSF membrane needs to be modified with such additives that show enhanced hydrophilic, conductive and permeation properties. The incorporation of zinc oxide (ZnO) nanoparticles into the PANI/PSF membrane significantly enhances its performance by improving membrane's hydrophilicity, reducing the adhesion of organic dyes and thereby increasing dye removal efficiency. Additionally, it modifies the membrane's microstructure, resulting in larger pore size and increased porosity, which facilitates better water transport and more effective dye adsorption. The interaction between PANI and ZnO also enhances the mechanical strength of the composite membrane, making it more robust under operational conditions, which is essential for consistent long-term performance. Furthermore, the combination of PANI and ZnO provides additional active sites for adsorption, improving the capture of dye molecules and heavy metal ions. The functional groups in both materials contribute to electrostatic

interactions that enhance the membrane's ability to reject metal ions effectively, leading to superior separation capabilities compared to membranes without ZnO.

This work introduces a novel polysulfone (PSF) composite membrane including polyaniline (PANI) and zinc oxide (ZnO) nanoparticles. The membrane is specifically engineered to efficiently eliminate heavy metal ions and dyes by means of simultaneous adsorption. The ZnO–(PSF/PANI) composite membrane is readily fabricated by incorporating ZnO into PANI–PSF membranes using the phase inversion approach under ambient environmental conditions. Subsequently, these membranes are subjected to a methodical analysis using UV-visible spectroscopy. Fourier transform infrared (FTIR) spectroscopy was shown to be quite useful in the analysis of the functional groups that are present in the synthesized membranes. The X-ray diffractometer (XRD) was used to analyze the chemical composition of the membrane surface, while contact angle measurement was used to assess its hydrophilic characteristics. The outer and cross-sectional textures of the membranes were observed using a scanning electron microscope (SEM). The performance evaluation involved assessing the membrane's porosity, solvent content, pure water flow rate and ability to reject BSA. The antifouling characteristic was verified by conducting ultrafiltration studies using BSA as a representative protein. The fabricated PPZ membranes presented a pragmatic method for boosting the fouling resistance of hybrid membranes and for improving permeability, and offered an innovative approach for efficient elimination of metal ions and dyes simultaneously from water.[32]

2. Experimental

2.1 Materials

Polysulfone (PSF) (average molecular weight 80 000 g mol^{-1}, density 1.24 g mL^{-1} at 25 °C, T_g 190 °C) (Sigma-Aldrich), aniline ($C_2H_5NH_2$) (Sigma-Aldrich), zinc nitrate ($Zn(NO_3)$) (Sigma-Aldrich), potassium permanganate ($KMnO_4$) (Sigma-Aldrich), ammonium persulphate (APS) (Sigma-Aldrich), *N*,*N*-dimethyl formamide (DMF), >99.0%, molecular weight 73.09 g mol^{-1}, density 0.944 g mL^{-1} at 25 °C, bp 153 °C (Sigma-Aldrich), acetic acid (CH_3COOH) (Sigma-Aldrich), hydrochloric acid (HCl) (Sigma-Aldrich), sulphuric acid (H_2SO_4) (Sigma-Aldrich), methylene blue (MB) (Sigma-Aldrich), sodium hydroxide (NaOH) (Sigma-Aldrich), methanol (CH_3OH) (Scharlu), propanol (C_3H_8O) (Scharlu), acetone (C_3H_6O) (Sigma-Aldrich) and ethanol (C_2H_5OH) (Sigma-Aldrich) were used.

2.2 Synthesis of PANI nanotubes

A solution designated as A was prepared by mixing 50 milliliters of distilled water with 1 milliliter of aniline monomer (0.2 M) in a flask and stirring the mixture for 45 minutes. In another flask, a mixture referred to as solution B was prepared by combining 50 mL of distilled water, 0.25 M ammonium persulfate (APS) and 2 mL of acetic acid, and then agitating the mixture for the same duration.[35] After 45 minutes, both solutions were combined and stirred for a further half an hour at room temperature. Thereafter, the combination was left unattended for a whole day.[36] After this time, a dark, green-colored product was transferred to a separating funnel containing 30 mL each of acetone and distilled water to eliminate any unreacted components. This separation process yielded two distinct layers; the predominant layer was collected and further washed with acetone and distilled water.[37] Subsequently, the collected layer was filtered using filter paper and the product was dried by exposure to air before undergoing PANI characterization.

2.3 Synthesis of ZnO nanorods

Initially, a 50 mL solution (labeled as solution A) containing 0.9 M NaOH in water was prepared and stirred for 30 minutes within the temperature range of 55–60 °C. Subsequently, a 50 mL solution of $Zn(NO_3)_2$ (0.45 M) in water was gradually introduced into solution A. The resultant mixture was allowed to settle for 24 hours at room temperature after being agitated for 90 minutes at a temperature of 55–60 °C. The reaction mixture was then allowed to settle for three hours without being stirred and the supernatant solution was then carefully discarded.[38] Upon the formation of a white precipitate, it was transferred to a separating funnel containing 30 mL of distilled water and ethanol for rinsing.[39] The collected precipitates were subjected to calcination in an oven at 80 degrees Celsius for 2 hours and were subsequently utilized for characterization purposes.

2.4 Synthesis of ZnO–(PANI/PSF) composite membranes

Due to their inherent hydrophobic nature and tendency for fouling, pristine PSF membranes have limited applications in water purification processes. To enhance their efficacy in the water treatment process, various types of hydrophilic additives are added. In this work, a very well-known hydrophilic nanofiller (ZnO)[40] is incorporated to enhance the hydrophilicity, antifouling character and pollutant rejection efficiency of the membranes. This incorporation is done by using the phase inversion method for varying concentrations from 0.05 to 0.3 wt%. A suitable amount of ZnO and PANI nanofiller was taken in a sample vial containing 3 mL of DMF and sonicated for 3 minutes by using a probe sonicator at 20 kHz and 100 W, and then transferred to the reaction mixture containing PSF for *in situ* membrane fabrication. The preparation of the PPZ membranes *via* the phase inversion method involves several key steps. First, a polymer solution is created by dissolving PSF in a solvent like *N*,*N*-dimethylformamide (DMF) at a concentration of 17.6 wt%, to which PANI and ZnO nanoparticles are added for uniform dispersion. This solution is then cast onto a flat support using a casting blade with a thickness typically between 100 and 300 micrometers. The cast film is immersed in a coagulation bath composed of approximately 70% water and 30% ethanol for a phase inversion time of 5 to 30 minutes, allowing for solvent exchange and the formation of a porous structure. Finally, the membrane is subjected to post-treatment, including washing with distilled water to remove residual solvents

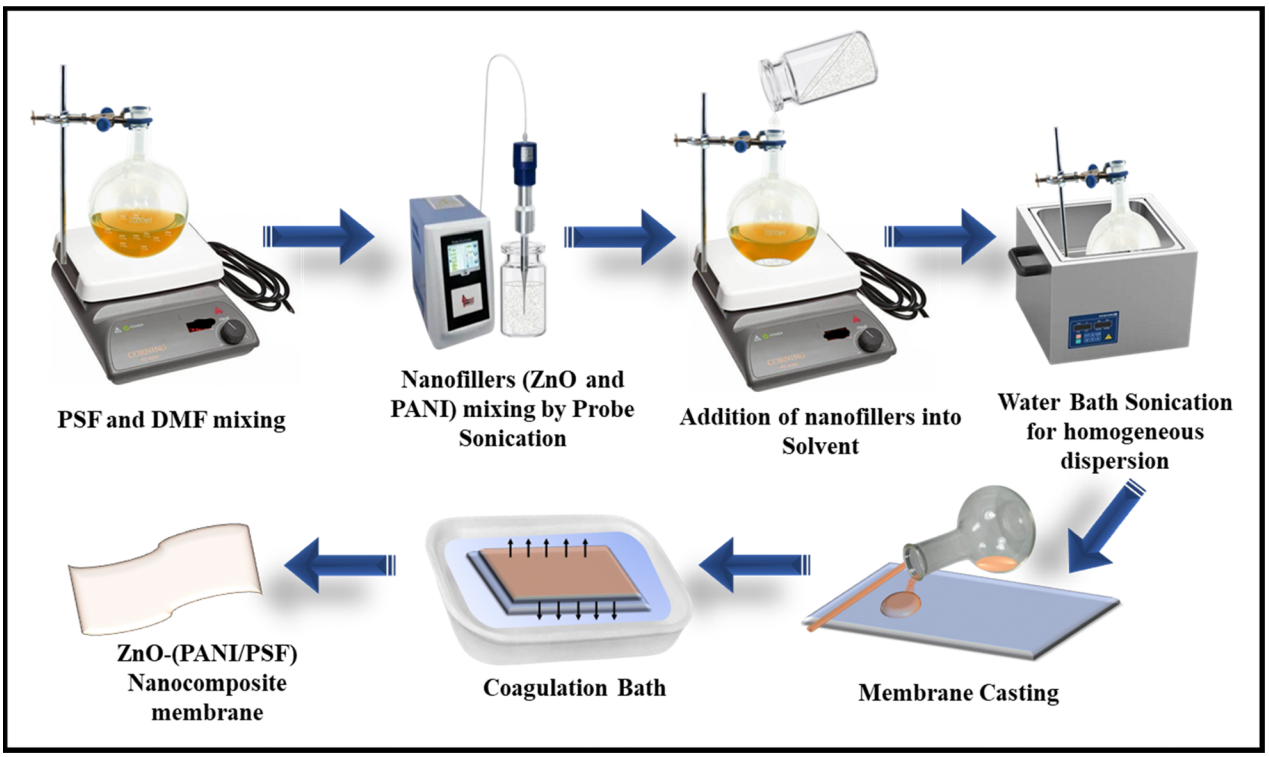

Fig. 1 Fabrication of ZnO–(PANI/PSF) composite membranes by phase inversion.

Table 1 Optimized compositions of ZnO/(PSF–PANI) nanocomposite membranes

S. no.	Codes	ZnO (wt%)	PSF (wt%)	PANI (wt%)	DMF (wt%)
1	PPZ 0	0	15	0	85
2	PPZ 0.05	0.05	14.7	0.25	85
3	PPZ 0.1	0.1	14.65	0.25	85
4	PPZ 0.15	0.15	14.6	0.25	85
5	PPZ 0.2	0.2	14.55	0.25	85
6	PPZ 0.25	0.25	14.5	0.25	85
7	PPZ 0.3	0.3	14.45	0.25	85

and drying under controlled conditions. In this way, different ZnO–(PSF/PANI) blend nanocomposite membranes were fabricated, as shown in Fig. 1, and their composition with their specific codes (PSF–polyaniline–ZnO = PPZ) is given in Table 1.

2.5 Adsorption studies

For adsorption studies of membranes towards cationic methylene blue as a model dye, PANI/PSF nanocomposite membranes are used. These experiments were conducted in 100 mL beakers containing 40 mL dye solution with 0.5 g of dye content. These samples were placed in an isothermal bath for 1 hour at room temperature. UV-visible spectroscopy was used to determine the initial and final concentration of dyes and metal ions.[41] Various factors, including pH and dye concentration with time, were also measured during dye adsorption investigations. Optimized pH for dyes was 3–11, time 0–24 h and concentration of dyes 20–200 mg L^{-1}. The following equation was used for adsorption measurement:

$$\text{Adsorption } (q_e) = \frac{(C_0 - C_e)}{m} \quad (1)$$

The concentration of dyes is represented by C_0 and the equilibrium concentration of dye is represented by C_e (mg L^{-1}), M is the mass of the composite membrane and V is the volume of the composite membrane.[42] The pH range (3–11) of dyes was adjusted with 0.1 M HCl and 0.1 M NaOH solutions and the dye concentration was 100 mg L^{-1}. In order to conduct the kinetic adsorption test, 0.5 g of ZnO–(PSF/PANI) composite membranes was dipped in various concentrations of dye solution and removed after predetermined amounts of time.[43] This experiment was repeated at room temperature and at 35 °C and 45 °C. The amount of adsorption at time t was then computed using the following equation:

$$\text{Adsorption } (q_t) = \frac{(C_0 - C_t)}{m} \quad (2)$$

The initial and equilibrium dye concentrations are denoted by C_0 and C_t (mg L^{-1}), respectively, and the composite membrane's mass is denoted by m.

2.6 Characterization

X-ray diffraction (XRD), Fourier transform infrared spectroscopy (FTIR), scanning electron microscopy (SEM), and atomic force microscopy (AFM) were among the characterization methods used in this investigation. A digital pH meter called the pH master dynamica was used to determine the pH of the

MB solution. ZnO, PANI, and PSF functional groups were analyzed using FTIR spectroscopy (ALPH 1 Bruker) in the 400–4000 cm^{-1} spectral region. To get information on crystallographic structure, X-ray diffraction (XRD) analysis was performed on fillers and composite membranes using a JEOL JDX-3532 X-ray diffractometer (JEOL, Tokyo, Japan) utilizing Cu Kα radiation. Scanning electron microscopy was used to study the morphology of PSF, PANI, and ZnO using a JSM5910 device (JEOL, Tokyo, Japan). The thermal stability of ZnO, synthesized PANI, and manufactured membranes was assessed by thermogravimetric analysis (Diamond series TG/DTA Perkin-Elmer, USA) across a temperature range of 40–800 °C. Atomic force microscopy (AFM) using a Nanosur Mobile scanning probe optical microscope (Switzerland) was used to assess the surface roughness of composite membranes.

2.7 Membrane performance/stability tests

2.7.1 Porosity. After being divided into 1 cm^2 pieces, the membranes were left in deionized water for a whole day. Both before and after soaking in water, the weight of the membrane was measured.[44]

Porosity was calculated using the following equation:

$$\text{Porosity } \% = \frac{(W_2 - W_1)\rho_1}{\rho_1 W_2 + (\rho_2 - \rho_1)W_1} \quad (3)$$

where W_1 = weight of the membrane before wetting, W_2 = weight of the membrane after wetting, ρ_2 (1 g cm^{-3}) = density of water, and ρ_1 (1.26 g cm^{-3}) = density of PSF.

2.7.2 Solvent content. A 1 cm^2 piece of the membranes was submerged in various solvents (water, methanol, ethanol, and propanol) for 24 hours. After this period, the weight of the membrane was recorded both before and after immersion in the solvents.[45]

The solvent content was calculated using the following equation:

$$\text{Solvent content } \% = \frac{W_2 - W_1}{W_2} \times 100 \quad (4)$$

where W_1 = weight of the membrane before wetting and W_2 = weight of the membrane after wetting.

2.7.3 Pure water flux. A membrane vacuum filtration pump was employed to evaluate the flow of clean water. The water permeability of both pure and composite membranes was measured. Following this, the membranes were immersed in distilled water for an entire day. After soaking, any excess water was removed from the surface of the membranes, which were then compacted by passing 5 liters of deionized water through them at a pressure of 0.1 MPa. The performance of the manufactured membranes was assessed based on the pure water flow per minute.[46]

The water flux was calculated using the following equation:

$$\text{Pure water flux } (J) = \frac{Q}{A_t} \quad (5)$$

where Q = permeate volume, t = time, and A = membrane surface area in cm^2.

2.7.4 Antifouling property. The antifouling properties of the membranes were assessed using bovine serum albumin (BSA) as the model protein.[47] Both the pristine and composite membranes were employed to filter a BSA solution with a concentration of 0.8 g L^{-1} at a pressure of 0.2 MPa for a duration of 40 minutes. The measurements J_{w_1} and J_{w_2} (in L m^{-2} h^{-1} bar^{-1}) were utilized to determine the flux recovery ratio (FRR).[33] The FRR is calculated using the following formula:

$$\text{FRR } \% = \frac{J_{w_1}}{J_{w_2}} \times 100 \quad (6)$$

J_{w_1} = initial water flux of the unfouled membrane, J_{w_2} = water flux of the washed membrane after fouling.

BSA rejection % values were measured by using the following formula:

$$\%\ R_{BSA} = \left(1 - \frac{C_p}{C_f}\right) \times 100 \quad (7)$$

The concentration of the penetrated BSA solution is represented by C_p, while the concentration of the feed BSA solution is represented by C_f.

In antifouling studies of ZnO–(PANI/PSF) membranes, surface flow rates are typically set around 20 L m^{-2} h^{-1}, with a standard cleaning duration of approximately 30 minutes. Common cleaning agents include 0.2 M NaOH and citric acid solutions, which effectively break down both organic and inorganic foulants.

2.7.5 Determination of dye rejection performance of ZnO–(PANI/PSF) NC membranes. To measure dye rejection, methylene blue (MB) dye and the actual sample were filtered through composite membranes using a filtration assembly. The vacuum filtration process utilizing a ZnO–(PANI/PSF) membrane for removing methylene blue (MB) dye typically involves specific parameters to optimize its effectiveness. MB dye concentration (10 mg L^{-1}) was used for testing. The process employs a vacuum pressure of approximately 75 kPa (563 mm Hg) to enhance filtration efficiency, and the vacuum is usually maintained for about 15 minutes. The concentration of the permeate and feed solutions was then measured using a UV-vis spectrophotometer.[48]

The following formula is used to determine the percentage of dye removal:

$$\%\ \text{Rejection of MB} = \left(\frac{C_{\text{permeate}}}{C_{\text{feed}}}\right) \times 100 \quad (8)$$

2.7.6 Determination of metal ion rejection performance of ZnO–(PANI/PSF) nanocomposite (NC) membranes. Due to the toxic effects of heavy metal ions on human health, their removal is necessary from wastewater. In this study, potassium permanganate ($KMnO_4$) containing manganese (VII), Mn^{7+}, is studied as a model heavy metal ion.[49] For heavy metal rejection experiment, aqueous solution of 50 mg L^{-1} (50 ppm) of $KMnO_4$ was prepared. This heavy metal ion (HMI) solution containing Mn^{7+} ions was filtered through all PANI/PSF and ZnO–(PANI/PSF)

NC membranes by using a vacuum pump at 0.03 MPa for 20 minutes each.[50] The UV-visible spectrophotometer was used to measure both initial and final concentrations of the filtrates at λ_{max} = 525 nm.

The following formula was used to measure the percentage of HMI removal:[51]

$$\%\ \text{Rejection of HMI} = \left(\frac{C_{\text{permeate}}}{C_{\text{feed}}}\right) \times 100 \qquad (9)$$

3. Results and discussion

3.1 Surface topographical analysis

The study utilized scanning electron microscopy (SEM) to examine both the pristine PSF membrane and the effects of incorporating ZnO nano fillers into the PANI/PSF composite membrane. Fig. 2 illustrates SEM images of PANI/PSF membranes containing varying concentrations of ZnO nanotubes. Fig. 1a shows that the pure PSF membrane has no obvious pores and has no disorganized and dense internal structure.[52] Fig. 2b shows the surface morphology of PPZ-0.05. The pore size of the PPZ-0.05 surface is 80 nm to 90 nm and the membrane surface is flat and smooth.[13,53] The shape and size of pores in PSF membranes can be affected by the presence of ZnO and PANI, which may also speed up the process of phase inversion.[54] PANI and ZnO have strong coordination with PSF which prevents the agglomeration of nanoparticles.[55] As shown in Fig. 2c, the pore size of the PPZ-0.1 membrane increases with increasing ZnO content.[56] The increased concentration of ZnO in the PPZ membranes from PPZ-0.15 to PPZ-0.2 also enhances their asymmetric structure with distinct macropores.[57] Agglomeration due to ZnO addition began and the number of pores decreased and pore size reduced. SEM images clearly indicate that these changes result from the formation of pores within the membrane structure. The increased hydrophilicity,[58] improved water flow and increased surface roughness of the membrane are believed to facilitate better dispersion of nanofillers (ZnO) within PANI/PSF.[59] Adding ZnO to PANI/PSF promotes nucleation and growth processes, thereby enhancing membrane roughness. Furthermore, the inclusion of ZnO/PANI in the polymer enhances the membrane's ability to resist fouling.

These images obtained from SEM reflect the effective filtering and adsorptive removal of MB dyes by employing membranes that are selective depending on the diameters of their pores.

3.2 Analysis of membrane structure, composition and physiochemical properties

The incorporation of ZnO at optimized concentrations into PANI/PSF was investigated using Fourier transform infrared (FTIR) spectroscopy in the range of 4000 to 400 cm^{-1} to analyze the presence of various functional groups on the membrane surface. The FTIR spectra were obtained for PANI (Fig. S2a, ESI†), ZnO (Fig S2b, ESI†), pristine PSF and the composite membranes PPZ-0.05, PPZ-0.1, PPZ-0.15, PPZ-0.2, PPZ-0.25 and PPZ-0.3.

The composite membranes displayed distinctive absorption bands, such as one at 871 cm^{-1} linked to the phenyl group,

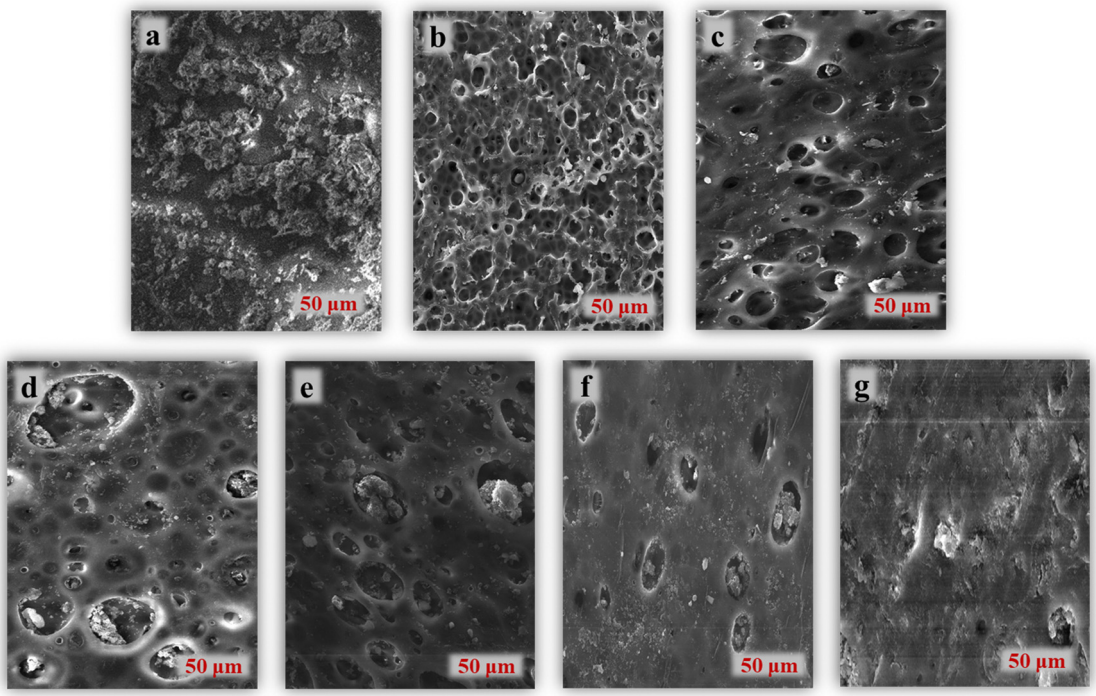

Fig. 2 SEM images of (a) pristine PSF, (b) PPZ-0.05, (c) PPZ-0.1, (d) PPZ-0.15, (e) PPZ-0.2, (f) PPZ-0.25, and (g) PPZ-0.3.

a benzoid ring stretching vibration band at 1252 cm^{-1} and a broad peak at 1401 cm^{-1} indicating N–H bending in polyaniline, confirming its presence and interaction with PSF.[34,60] Moreover, when a moderate amount of ZnO is added (PPZ-0.05), no shoulder peaks or peak shifting occurs, but in composite membranes with higher ZnO content (PPZ-0.1 to PPZ-0.3), the O–H stretching peak shifts from 3499 cm^{-1} to 3428 cm^{-1} due to surface hydroxyl groups[61] on ZnO, indicating increased hydrogen bonding with PANI and PSF. This can broaden and shift O–H and N–H stretching vibrations.[62,63] Furthermore, the absorption bands related to sulfone groups in PSF show minor shifts and changes in intensity, while a peak at 1280 cm^{-1} confirms agglomeration within the composite membranes due to higher ZnO content.[62,64]

These findings highlight the significant impact of incrementally adding ZnO to the PANI/ZnO/PSF composite membrane. Extreme concentrations of ZnO in PANI/PSF composite membranes induce agglomeration,[56] impeding polymer chain mobility and causing steric hindrance, thereby compromising effective bonding and risking phase separation. Agglomerated ZnO clusters in membranes obstruct water passage, reducing permeability and yielding uneven permeation. These clusters diminish water flow, reducing permeance and affecting membrane functionality. Additionally, elevated surface roughness enhances hydrophobicity, increasing the contact angle and negatively affecting uniformity and properties of the composite membranes.

Compositional and structural analysis of ZnO, PANI, pristine PSF and as-synthesized ZnO–(PANI/PSF) membranes of all composition was done with the help of X-ray diffractogram. Fig. S3 (ESI†) shows the XRD of ZnO and PANI. The XRD of pristine PSF and nanocomposite membranes PPZ-0.05, PPZ-0.1, PPZ-0.15, PPZ-0.2, PPZ-0.25, and PPZ-0.3 is shown in Fig. 3b. PSF exhibited a broad peak ranging from 12° to 24°, corresponding to amorphous structure of the PSF membrane.[65] For the nanocomposite membranes, no additional peaks were observed except the characteristic diffraction for hexagonal ZnO and PANI.

3.3 Membrane permeation properties

Using a gravimetric approach, the porous nature of the nanocomposite membranes was evaluated.[66] Initially, the membranes were weighed, soaked in water for 24 hours and then tested. The introduction of hydrophilic polyaniline (PANI) and ZnO nanoparticles to PSF membranes notably increased their porosity, as depicted in Fig. 4a. The use of nano-fillers, which created holes in the polymer matrix during the phase inversion manufacturing process, is attributed to this enhancement. On the other hand, membrane porosity was reduced when ZnO nanoparticle concentration was increased from 0.05 weight percent to 0.3 weight percent, possibly as a result of pore obstruction.[67] Because of the swelling of the polymers, the addition of ZnO nanoparticles further increased the thickness of the membrane. More specifically, for the PPZ-0.3 membrane with the highest nanoparticle loading, the thickness increased from 100 μm for the pristine PSF to 120 μm. Overall transport resistance was not considerably affected by swelling, even with this increase in thickness.[68]

The integration of nanoparticles into PSF membranes influenced their porosity.[63] Pristine PSF exhibited a porosity percentage of 75.5%, which increased to 77% with PANI addition. Within the ZnO–(PANI/PSF) ternary composite membrane, adding ZnO nanoparticles (NPs) further increased the porosity to 80% for PPZ-0.05. However, as ZnO NP content went up from 0.1 to 0.3, porosity gradually declined to 57% due to nanoparticle clustering.[69]

The ZnO–(PANI/PSF) membrane showed outstanding stability and durability in acidic and basic medium, as confirmed by consistent FTIR results pre and post exposure to acidic solutions with subsequent washing.[70] This confirms that there was no leakage of PANI or ZnO from the membrane matrix, validating its structural integrity and resilience against extreme chemical conditions. The successful blending of ZnO–(PANI/PSF)components further accentuates the membrane's stability and ability to endure severe pH environments without compromising its physiochemical traits.[71]

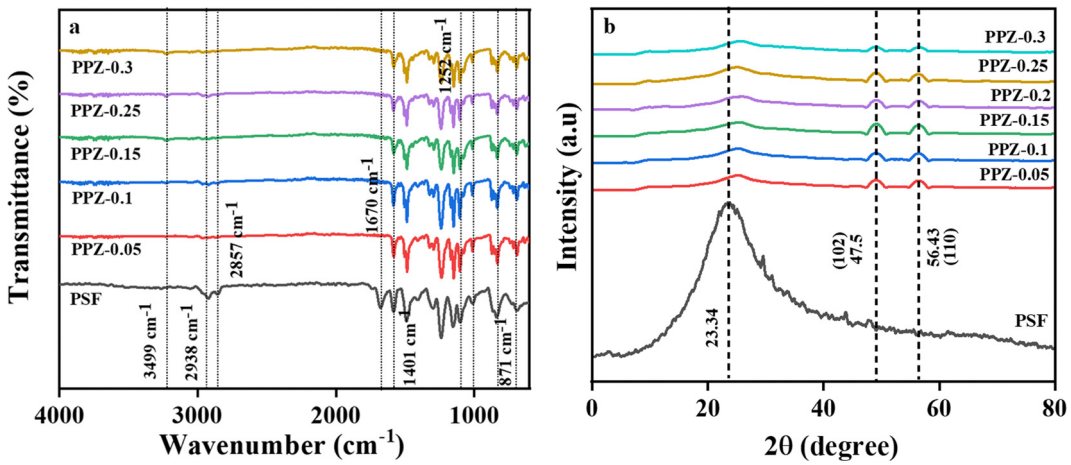

Fig. 3 (a) FTIR spectra of pristine PSF and composite membranes PPZ-0.05, PPZ-0.1, PPZ-0.15, PPZ-0.25, and PPZ-0.3. (b) X-ray diffractogram of pristine PSF and composite membranes PPZ-0.05, PPZ-0.1, PPZ-0.15, PPZ-0.25, and PPZ-0.3.

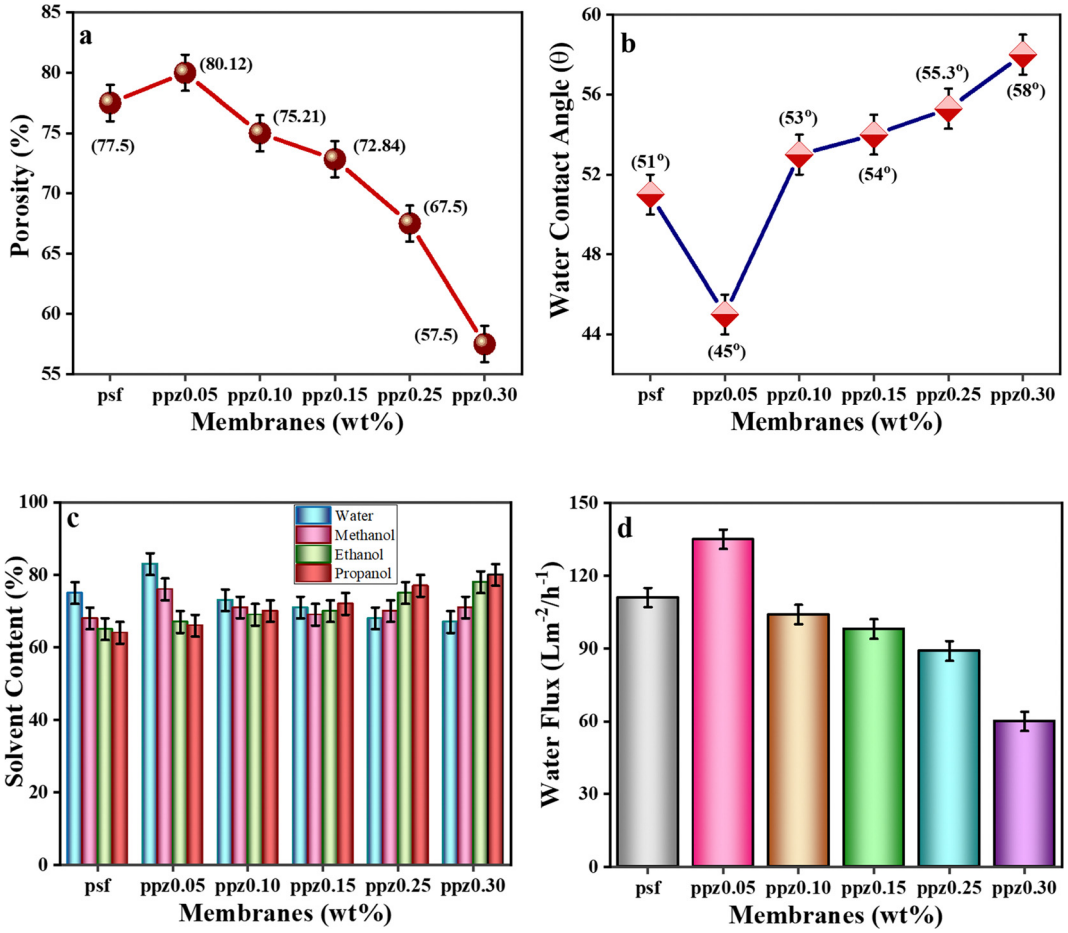

Fig. 4 (a) Porosity, (b) water contact angle, (c) solvent content, and (d) pure water flux.

Fig. 4b depicts the water contact angle study. The water contact angle measurements show how hydrophilic the composite membranes are. Lower WCA values mean better hydrophilicity,[72] which helps prevent membrane fouling.[73] Adding PANI/ZnO to the membranes made the WCA go down from 51.5° to 45° for the PPZ-0.05 sample, making the membrane easier to wet. But as more PANI/ZnO was added, the WCA went up slowly, reaching 60° for samples PPZ-0.1 to PPZ-0.3. The –NH groups of PANI and the functional groups of ZnO helped reduce the natural hydrophobicity of PSF, aiding in solvent adsorption and filtration.[74] However, this positive impact lessened with higher amounts of PANI/ZnO included.[75]

Solvent absorption tests (Fig. 4c) using four different solvents with different polarity indicated that an increase in filler content improved water permeability and hydrophilicity.[76] However, due to particle aggregation, subsequent incorporation of ZnO nanoparticles resulted in a shift towards hydrophobic behavior, improving the material's antifouling and adsorption properties.[70,76]

In Fig. 4d, with the addition of 0.05 weight percent ZnO to PANI/PSF membranes, the pure water flux (PWF) of the modified membranes was significantly enhanced by improving the water flux rate and adsorption and filtration capabilities.[77] Conversely, higher concentrations of ZnO (0.1 wt% to 0.3 wt%) resulted in pore blockage, which negatively impacted the PWF by reducing the membrane's permeability.

The results show that a considerable increase in water flux occurs in PPZ-0.05 when there is a combination of lower water contact angle and higher porosity.[78] The fact that greater water permeability becomes feasible by the increased porosity and faster water flow through the membrane is shown by the reduced contact angle, which also implies improved membrane wettability.[79] The importance of optimising membrane characteristics for effective water transport applications is highlighted by this synergistic effect.[13,80]

3.4 BSA resistance and antifouling characteristics of nanocomposite membranes ZnO–(PANI/PSF)

Membrane fouling and flux reduction are significant challenges in membrane technology due to the build-up of solute particles during filtration. One effective approach to combat fouling is enhancing membrane hydrophilicity by adding hydrophilic fillers.[81] In this study, the addition of ZnO nanofillers to PANI/PSF membranes increased hydrophilicity and reduced fouling. Experimental filtration was conducted using composite membranes and bovine serum albumin (BSA) as a fouling agent.[82] The flux recovery ratio demonstrated the efficacy of the

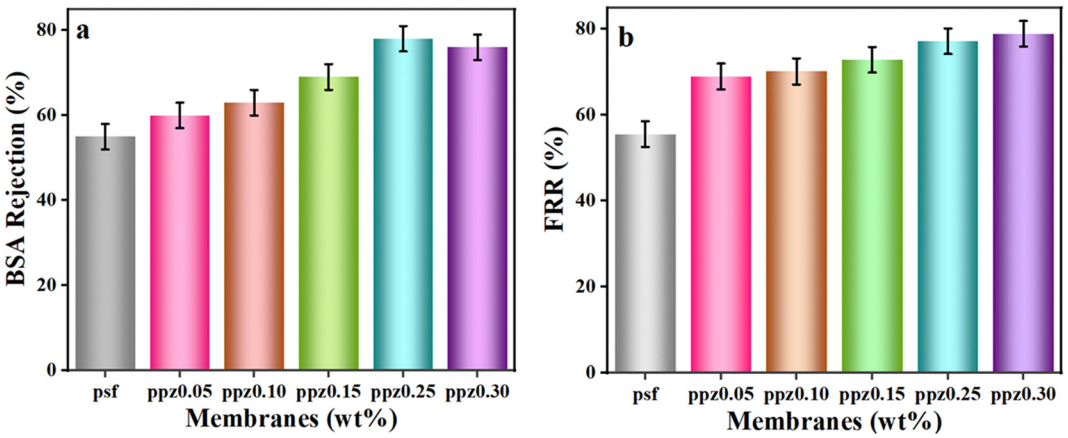

Fig. 5 (a) Protein rejection of pristine PSF and composite membranes PPZ-0.05, PPZ-0.1, PPZ-0.15, PPZ-0.25, and PPZ-0.3. (b) Flux recovery ratio of pristine PSF and composite membranes PPZ-0.05, PPZ-0.1, PPZ-0.15, PPZ-0.25, and PPZ-0.3.

composite membranes in lowering fouling and enhancing flux recovery both before and after the BSA solution was filtered.[83]

Fig. 5a demonstrates a significant improvement in BSA rejection as nanofillers are gradually incorporated into the hydrophobic PSF membrane.[84] Because it is hydrophobic, pure PSF has a low protein rejection rate of about 57%. However, the rejection rate increases to 60% when ZnO is added gradually at a weight percentage of 0.05, a trend that is further emphasized in the PPZ-0.15 and PPZ-0.25 membranes, where rejection rates vary from 69% to 78%. In the case of the PPZ-0.3 membrane, there is a slight decrease to 76% due to agglomeration leading to pore blocking resulting from improper distribution of ZnO nanofillers within the membrane.[85] BSA molecules show less deposition on ZnO incorporated membranes as they tend to adsorb more easily on hydrophobic surfaces rather than hydrophilic surfaces. Therefore, the presence of ZnO nanotubes in the membranes hinders the adsorption of BSA, making the membranes more hydrophilic. The flux recovery ratio (FRR) values of all membranes are higher compared to the pristine PSF membrane (Fig. 5a). A higher FRR value (Fig. 5b) indicates better antifouling properties of the membranes. It is worth noting that FRR values increase with the presence of ZnO nanotubes. The PSF membrane without any ZnO concentration exhibits the lowest FRR value due to hydrophobic interactions between PSF and protein molecules.[86] However, membranes containing ZnO and PANI show improved fouling resistance, suggesting that protein molecules adsorbed during BSA filtration can be easily removed when flushed with water. Based on FRR values and water flux measurements, it is evident that membranes incorporating ZnO and PANI exhibit superior antifouling properties compared to pristine membranes. The enhanced antifouling ability can be attributed to the increased hydrophilicity resulting from ZnO presence. The combination of ZnO and PANI effectively prevents protein adsorption on surfaces due to the presence of hydrophilic functional groups.[87]

3.5 Performance evaluation of membranes

Practical applicability of ZnO–(PANI/PSF) membranes was investigated for simultaneous removal of organic dyes (decolorization) and heavy metal ions (desalination) from wastewater. MB dye is used as a model dye to test membrane removal efficiency and potassium permanganate ($KMnO_4$) containing manganese(VII) (Mn^{7+}) is studied as a model heavy metal ion.

3.5.1 Dye rejection studies of ZnO–(PANI/PSF) NC membranes. It is clear from Fig. 6 that the pristine PSF membrane is unable to remove MB dye efficiently from water as compared to PANI–PSF NC membranes and ZnO incorporated PANI–PSF membranes. Dye removal efficiency of the pristine PSF membrane is 67.5%[88] which is increased up to 91.2% when PANI is incorporated in the PSF membrane. This trend is further enhanced when a small amount of ZnO is added in PANI–PSF membranes, wherein the removal efficiency reaches up to 95.18%. Both ZnO and PANI are hydrophilic and responsible for the increased surface area of the NC membranes. Addition of PANI in PSF membranes increased the surface area of membranes and provided greater number of binding sites (amine and imine nitrogen).[88,89] As a result, strong electrostatic interactions were generated between PANI–PSF membranes and MB molecules which increases the removal effectiveness of PANI–PSF membranes. Hydroxyl groups and O^{2-} ions present on the surface of ZnO nanotubes[90] when incorporated into PANI–PSF membranes further enhanced the removal efficiency of membranes (*i.e.* 95.18%).

3.5.2 Heavy metal ion (HMI) rejection studies of ZnO–(PANI/PSF) NC membranes. Specific $KMnO_4$ solution was filtered through these membranes and the concentration present in feed and permeate solutions was determined by using a double beam UV-visible photo spectrophotometer at a wavelength of 525 nm. The results of these experiments are shown in Fig. 7. It can be concluded from heavy metal ion removal results by PSF/PANI NC membranes that the pristine PSF membrane shows 67% removal while upon PANI nanotube incorporation, HMI (heavy metal ion) removal efficiency increased maximum up to 94.3% by the PP 0.25 membrane.[91] HMI removal by PANI/PSF membranes is due to the presence of lone pairs present on oxygen atoms and (imine and amine) nitrogen atoms having lone pairs which show increased interaction toward heavy metal ions.[92] A slight increase in %age removal

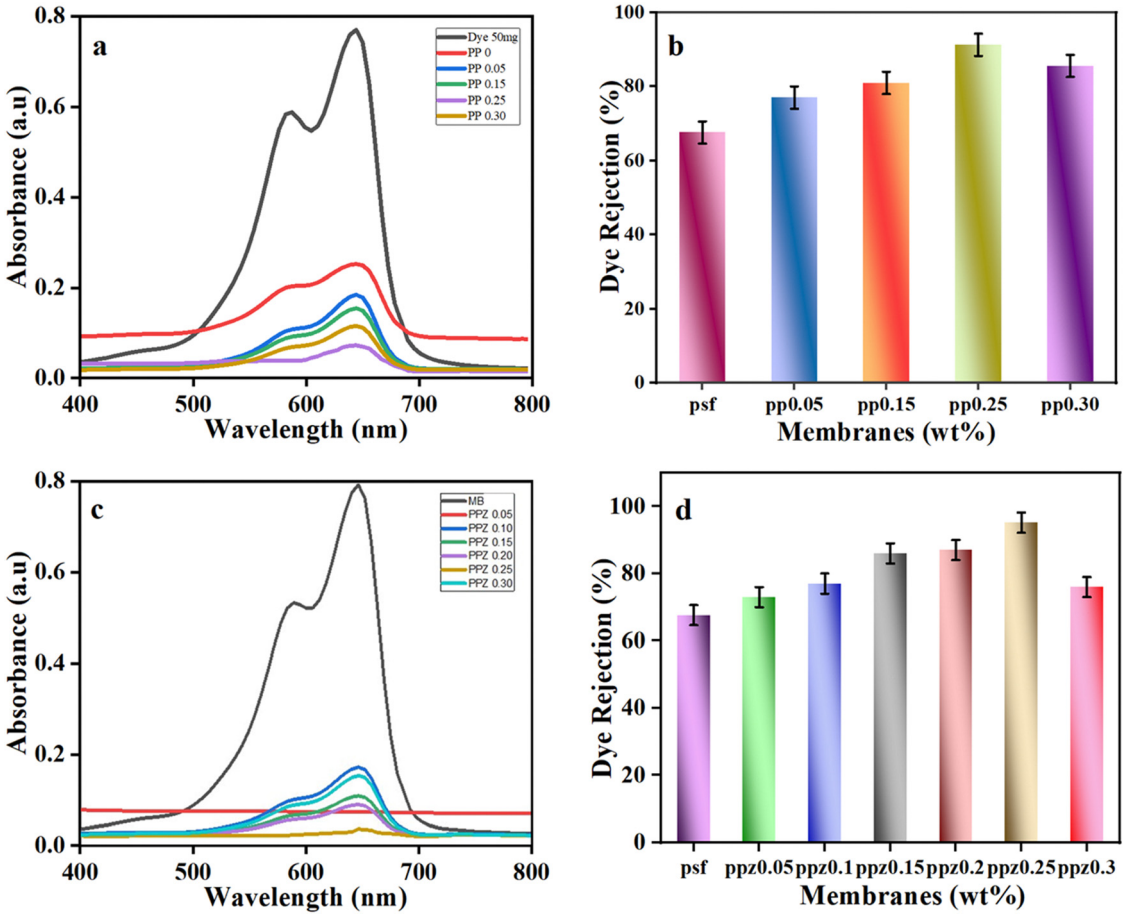

Fig. 6 (a) Absorbance spectra of MB dye rejection of pristine PSF and PANI composite membranes PP-0.05, PP-0.15, PP-0.25, and PP-0.3, (b) MB dye rejection of pristine PSF and PANI composite membranes PP-0.05, PP-0.15, PP-0.25, and PP-0.3, (c) absorbance spectra of MB dye rejection of pristine PSF and (ZnO/PANI) nanocomposite membranes PPZ-0.05, PPZ-0.1, PPZ-0.15, PPZ-0.25, and PPZ-0.3, and (d) MB dye rejection of pristine PSF and (ZnO/PANI) nanocomposite membranes PPZ-0.05, PPZ-0.1, PPZ-0.15, PPZ-0.25, and PPZ-0.3.

efficiency was seen when ZnO nanofillers were incorporated in PANI–PSF NC membranes. This improved removal efficiency from 94.3% to 96.21% for PPZ-0.15 is due to hydroxyl groups present on the ZnO nanorod structure.[90]

3.6 Proposed mechanism for ZnO–(PANI/PSF) NC membranes

ZnO–(PSF/PANI) membranes are effective for removing contaminants like methylene blue (MB) and manganese (Mn^{7+}) ions from contaminated water, simultaneously. Various forces of interaction cause ZnO and PANI to disperse uniformly when they are incorporated in the PSF. PSF has sulfone groups (–SO_2–) within its polymer backbone. These sulfone groups act as hydrogen bond acceptors because the sulfur atom, bonded to two oxygens, creates a region of partial negative charge.[93] ZnO surfaces have hydroxyl groups (–OH) due to the reaction of ZnO with moisture or hydroxide ions. These hydroxyl groups act as hydrogen bond donors because the hydrogen atom of the hydroxyl group is partially positively charged.[94] When ZnO and PSF come in contact, the hydrogen atoms of the hydroxyl groups on ZnO form hydrogen bonds with the oxygen atoms of the sulfone groups on PSF as illustrated in Fig. 8.[95] Moreover, when PANI is incorporated into the PSF matrix, the alignment and orientation of the functional groups facilitate the formation of hydrogen bonding.[30] The hydrogen atoms on the amino groups of PANI also form hydrogen bonds with the oxygen atoms in the sulfone groups of PSF. This occurs when the hydrogen bond donor (the –NH_2 group of PANI) interacts with the hydrogen bond acceptor (the –SO_2– or –O– groups of PSF). Along with hydrogen bonding, π–π interactions also dominate.[96] Both PSF and PANI contain aromatic structures. PSF has benzene rings in its backbone, while PANI has aniline rings.[97] These aromatic rings possess π-electron clouds that can interact with each other. In π–π interactions, aniline rings of PANI align parallel to the benzene rings of PSF. This parallel alignment allows for overlapping π-electron clouds, which leads to a stabilizing interaction between PANI and PSF. These interactions help to create a more integrated membrane structure and enhance the compatibility and adhesion between nanofillers and PSF, leading to better dispersion of ZnO and PANI within the PSF matrix.[98] Thus, improved interaction improves the mechanical properties, stability and performance of the nanocomposite PSF membrane.

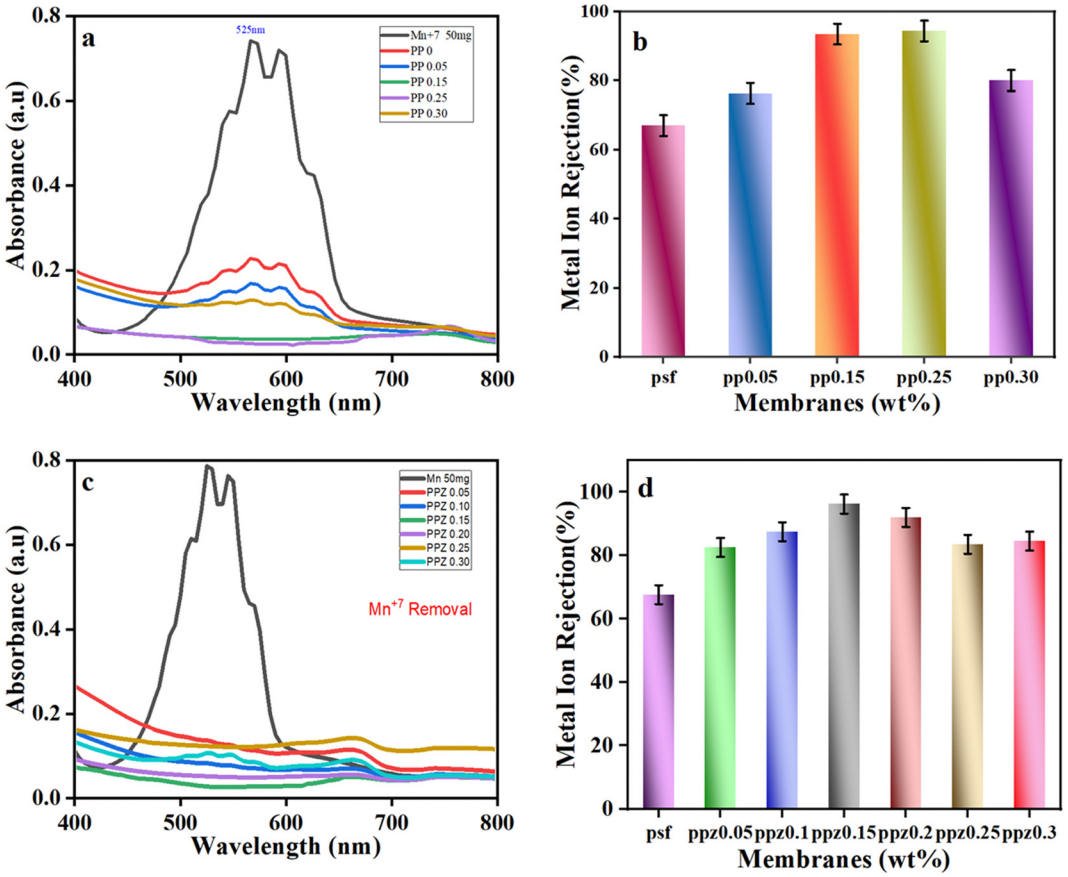

Fig. 7 (a) Absorbance spectra of Mn^{7+} ion rejection of pristine PSF and PANI composite membranes PP-0.05, PP-0.15, PP-0.25, and PP-0.3, (b) Mn^{7+} ion rejection of pristine PSF and PANI composite membranes PP-0.05, PP-0.15, PP-0.25, and PP-0.3, (c) absorbance spectra of Mn^{7+} ion rejection of pristine PSF and (ZnO/PANI) nanocomposite membranes PPZ-0.05, PPZb-0.1, PPZ-0.15, PPZ-0.25, and PPZ-0.3, and (d) Mn^{7+} ion rejection of pristine PSF and (ZnO/PANI) nanocomposite membranes PPZ-0.05, PPZ-0.1, PPZ-0.15, PPZ-0.25, and PPZ-0.3.

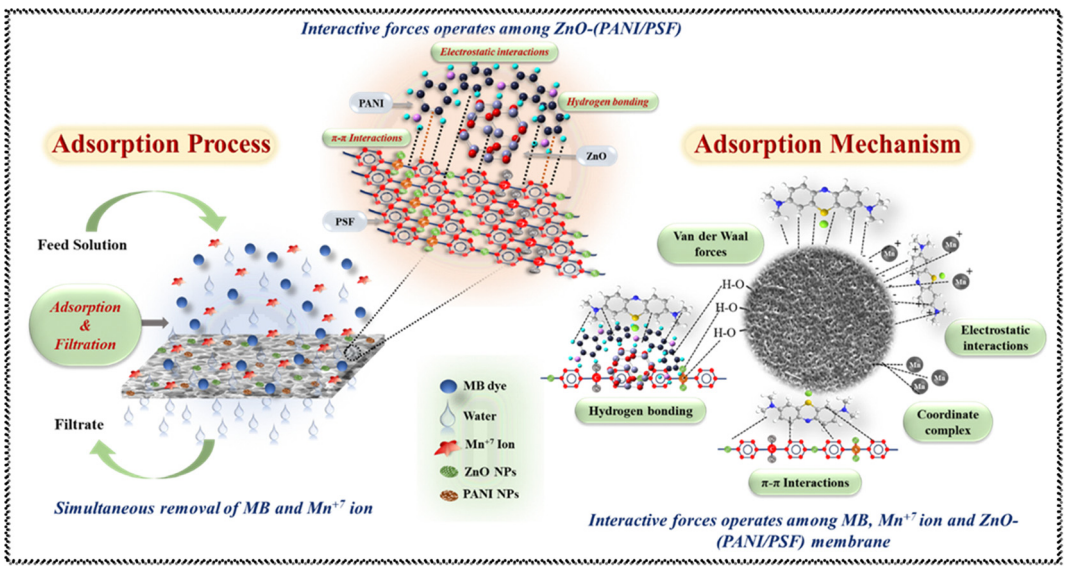

Fig. 8 Proposed mechanism for PPZ nanocomposite membranes.

When contaminated water having MB dye and Mn^{7+} metal ions is passed through ZnO–(PANI/PSF) nanocomposite membranes, some interactive forces are generated between contaminants and the ZnO–(PANI/PSF) nanocomposite membrane facilitating

adsorption and resulting in efficient removal of contaminants from polluted water.[99] MB is a cationic dye; the positively charged dye molecules are attracted to the negatively charged or neutralized regions on PANI, leading to effective adsorption.[100,101] PANI also contains aromatic rings in its structure. These rings can engage in π–π stacking interactions with the aromatic structures in MB. The conjugated π-electron systems of both PANI and MB can interact, facilitating the adsorption of MB onto PANI. The PSF membrane fabricated with ZnO nanoparticles and PANI possesses numerous active sites and a substantial surface area, which allows it to adsorb MB dye. This process involves physical adsorption, where van der Waals forces and electrostatic interactions secure the dye molecules to the membrane surface.[68] Meanwhile, Mn^{7+} ions in the solution tend to adsorb on the membrane surface by forming coordinate bonds with ZnO and PANI. The ZnO surface is negatively charged in neutral and basic solution, attracting the Mn^{7+} (positively charged) ions electrostatically to the membrane surface.[83] Additionally, the hydroxyl groups (–OH) on the ZnO surface can coordinate with Mn^{7+} ions. Mn^{7+} ions, being highly oxidizing and having a strong affinity for electron-pair donors, can form coordinate bonds with the electron pairs on the hydroxyl groups. This interaction helps to stabilize the Mn^{7+} ions on the ZnO surface.[102] ZnO can also form more complex structures through direct coordination. The ZnO surface creates a binding site for Mn^{7+} ions where the Mn^{7+} ions interact with the oxygen atoms of the ZnO lattice or with the hydroxyl groups attached to the surface.[103] The interaction between ZnO and Mn^{7+} ions can lead to the formation of surface complexes, where Mn^{7+} ions are bound to the ZnO surface through both electrostatic and coordination interactions. These complexes can alter the solubility and chemical reactivity of the Mn^{7+} ions, aiding in their removal from the aqueous solution. When Mn^{7+} ions contact the surface of the ZnO–(PANI/PSF) membrane, they can form surface complexes through electrostatic and coordination interactions. Electrostatic interactions occur when negatively charged ZnO attracts positively charged Mn^{7+} ions, leading to their binding. Additionally, Mn^{7+} ions can coordinate with oxygen atoms on the ZnO surface, sharing or transferring electron pairs to create a more stable complex. This binding significantly reduces the solubility of Mn^{7+} ions in solution, effectively removing them from the aqueous phase and decreasing their concentration. The interaction with ZnO also influences the chemical reactivity of Mn^{7+} ions, potentially stabilizing them and making them less reactive or altering their reactivity based on the surrounding conditions. Ultimately, these interactions enhance the removal efficiency of Mn^{7+} ions during processes like filtration or adsorption by preventing them from remaining in solution. Hence, the combination of electrostatic forces, π–π interactions and coordinate complex formation with the ZnO–(PANI/PSF) membrane enhances the membrane's adsorption capacity, attracting and holding dye molecules and heavy metal ions for effective removal from water. The PSF matrix provides structural support, while PANI and ZnO's unique adsorption properties contribute to a composite membrane with enhanced performance for MB dye removal.

4. Conclusion

The goal of this work was to enhance water filtration efficiency of hydrophobic polysulfone (PSF) membranes with the addition of zinc oxide (ZnO) and polyaniline (PANI). The optimal mixture was discovered to be 0.5 weight percent ZnO–(PANI/PSF). This alteration improved membranes' capacity to simultaneously absorb impurities and filter dyes.

The principal conclusions are as follows:

1. In comparison to pure PSF membranes, ternary composite membranes exhibited decreased shrinkage and increased surface roughness, which improved dye adsorption and filtering.

2. By adding ZnO and PANI, the membranes' hydrophilicity was enhanced, resulting in a decline in the water contact angle from 51.5° to 45°.

3. The water flow improved from 111 to 135 L m^{-2} h^{-1} bar^{-1}, and the BSA rejection rate increased from 57% to 78%.

4. Ternary composite membranes showed notable efficacy in rejecting the Mn^{7+} metal ion (96.21%) and MB dye (95.18%).

These results indicate that the developed membranes can effectively remove metal ions and dyes from wastewater at an affordable cost. The membranes' dual function of adsorption and filtration can enhance water quality and prolong membrane life, which makes them appropriate for real-world water treatment applications.

Author contributions

Aqsa Zahid: conceptualization, visualization, methodology, data curation, formal analysis, investigation, writing – original draft, writing – review & editing. Hafiza Hifza Nawaz: data curation, validation, formal analysis, resources, review & editing. Amna Siddique: writing – original draft, data curation and presentation. Basheer Ahmed: writing – original draft, data curation and presentation. Shumaila Razzaque: guidance, organization, reviewing and editing. Xuqing Liu: formal analysis, validation. Humaira Razzaq: conceptualization, supervision, visualization, project administration, formal analysis, validation, resources, funding acquisition, writing – review & editing. Muhammad Umar: conceptualization, supervision, visualization, project administration, formal analysis, resources, writing – review & editing.

Data availability

The data supporting this article have been included as part of the ESI.†

Conflicts of interest

The authors declare that they have no known competing financial interests or personal relationships that could have appeared to influence the work reported in this paper.

Acknowledgements

The authors express their gratitude to the Department of Chemistry, University of Wah, Pakistan, for the provision of lab facility. The authors acknowledge financial support from the Higher Education Commission of Pakistan through the NRPU Project by HEC Ref No. 20-15431/NRPU/R&D/HEC/2021. This research work was also supported by a grant from the Global Challenge Research Fund (GCRF), UK Research Innovation, and the Henry Royce Institute for Advanced Materials, funded through EPSRC grants EP/R00661X/1, EP/P025021/1, and EP/P025498/1.

References

1 C. V. Nachiyar, A. Rakshi, S. Sandhya, N. B. D. Jebasta and J. Nellore, Developments in treatment technologies of dye-containing effluent: a review, *Case Stud. Chem. Environ. Eng.*, 2023, 100339.
2 R. Megha, V. Lakhani, S. Vala, S. Dharaskar, N. R. Paluvai and M. K. Sinha, *et al.*, Removal of heavy metals and dyes from its aqueous solution utilizing metal organic frameworks (MOFs), *Mater. Today: Proc.*, 2023, **77**, 188–200.
3 A. Nishat, M. Yusuf, A. Qadir, Y. Ezaier, V. Vambol and M. I. Khan, *et al.*, Wastewater treatment: a short assessment on available techniques, *Alexandria Eng. J.*, 2023, **76**, 505–516.
4 Y. Lei, J. Zhao, H. Song, F. Yang, L. Shen and L. Zhu, *et al.*, Enhanced adsorption of dyes by functionalized UiO-66 nanoparticles: adsorption properties and mechanisms, *J. Mol. Struct.*, 2023, **1292**, 136111.
5 H. Solayman, M. A. Hossen, A. Abd Aziz, N. Y. Yahya, K. H. Leong and L. C. Sim, *et al.*, Performance evaluation of dye wastewater treatment technologies: a review, *J. Environ. Chem. Eng.*, 2023, **11**, 109610.
6 J. F. Nure and T. T. Nkambule, The recent advances in adsorption and membrane separation and their hybrid technologies for micropollutants removal from wastewater, *J. Ind. Eng. Chem.*, 2023, **126**, 92–114.
7 A. H. Birniwa, S. Habibu, S. S. A. Abdullahi, R. E. A. Mohammad, A. Hussaini and H. Magaji, *et al.*, Membrane technologies for heavy metals removal from water and wastewater: a mini review, *Case Stud. Chem. Environ. Eng.*, 2023, 100538.
8 E. S. Gad, M. E. Ali, A. A. Sammak, E. M. Elnaggar and S. F. A. Ali, Performance of Nanocomposite Polysulfone–Polyaniline Substrates for Enhanced Thin Film Membranes, *Egypt. J. Chem.*, 2022, **65**, 543–550.
9 A. Sahu, R. Dosi, C. Kwiatkowski, S. Schmal and J. C. Poler, Advanced polymeric nanocomposite membranes for water and wastewater treatment: a comprehensive review, *Polymers*, 2023, **15**, 540.
10 R. Singh, M. Singh, N. Kumari, S. J. Maharana and P. Maharana, A comprehensive review of polymeric wastewater purification membranes, *J. Compos. Sci.*, 2021, **5**, 162.
11 H. Ravishankar, J. Christy and V. Jegatheesan, Graphene oxide (GO)-blended polysulfone (PSf) ultrafiltration membranes for lead ion rejection, *Membranes*, 2018, **8**, 77.
12 S. C. Mamah, P. S. Goh, A. F. Ismail, N. D. Suzaimi, L. T. Yogarathinam and Y. O. Raji, *et al.*, Recent development in modification of polysulfone membrane for water treatment application, *J. Water Process Eng.*, 2021, **40**, 101835.
13 A. Alkhouzaam and H. Qiblawey, Novel polysulfone ultrafiltration membranes incorporating polydopamine functionalized graphene oxide with enhanced flux and fouling resistance, *J. Membr. Sci.*, 2021, **620**, 118900.
14 T.-Y. Liu, R.-X. Zhang, Q. Li, B. Van der Bruggen and X.-L. Wang, Fabrication of a novel dual-layer (PES/PVDF) hollow fiber ultrafiltration membrane for wastewater treatment, *J. Membr. Sci.*, 2014, **472**, 119–132.
15 G. S. Ibrahim, A. M. Isloor, A. M. Asiri, A. Ismail, R. Kumar and M. I. Ahamed, Performance intensification of the polysulfone ultrafiltration membrane by blending with copolymer encompassing novel derivative of poly(styrene-*co*-maleic anhydride) for heavy metal removal from wastewater, *Chem. Eng. J.*, 2018, **353**, 425–435.
16 X. Wu, Z. Xie, H. Wang, C. Zhao, D. Ng and K. Zhang, Improved filtration performance and antifouling properties of polyethersulfone ultrafiltration membranes by blending with carboxylic acid functionalized polysulfone, *RSC Adv.*, 2018, **8**, 7774–7784.
17 M. S. Rameetse, O. Aberefa and M. O. Daramola, Effect of loading and functionalization of carbon nanotube on the performance of blended polysulfone/polyethersulfone membrane during treatment of wastewater containing phenol and benzene, *Membranes*, 2020, **10**, 54.
18 B. S. Al-Anzi and O. C. Siang, Recent developments of carbon based nanomaterials and membranes for oily wastewater treatment, *RSC Adv.*, 2017, **7**, 20981–20994.
19 R. Rezaee, S. Nasseri, A. H. Mahvi, R. Nabizadeh, S. A. Mousavi and A. Rashidi, *et al.*, Fabrication and characterization of a polysulfone-graphene oxide nanocomposite membrane for arsenate rejection from water, *J. Environ. Health Sci. Eng.*, 2015, **13**, 1–11.
20 L. Badrinezhad, S. Ghasemi, Y. Azizian-Kalandaragh and A. Nematollahzadeh, Preparation and characterization of polysulfone/graphene oxide nanocomposite membranes for the separation of methylene blue from water, *Polym. Bull.*, 2018, **75**, 469–484.
21 Y. Kang, M. Obaid, J. Jang, M.-H. Ham and I. S. Kim, Novel sulfonated graphene oxide incorporated polysulfone nanocomposite membranes for enhanced-performance in ultrafiltration process, *Chemosphere*, 2018, **207**, 581–589.
22 M. Kumar, Z. Gholamvand, A. Morrissey, K. Nolan, M. Ulbricht and J. Lawler, Preparation and characterization of low fouling novel hybrid ultrafiltration membranes based on the blends of GO-TiO_2 nanocomposite and polysulfone for humic acid removal, *J. Membr. Sci.*, 2016, **506**, 38–49.
23 Y. Qi, L. Zhu, X. Shen, A. Sotto, C. Gao and J. Shen, Polythyleneimine-modified original positive charged nanofiltration

membrane: removal of heavy metal ions and dyes, *Sep. Purif. Technol.*, 2019, **222**, 117–124.
24 M. Yan, Y. Xi, N. Jiang, Q. Li, S. Zheng and Y. Hu, *et al.*, High-performance thin film composite forward osmosis membrane for efficient rejection of antimony and phenol from wastewater: characterization, performance, and MD-DFT simulation, *J. Membr. Sci.*, 2024, **703**, 122847.
25 A. Samadi, Z. Wang, S. Wang, S. Nataraj, L. Kong and S. Zhao, Polyaniline-based adsorbents for water treatment: roles of low-cost materials and 2D materials, *Chem. Eng. J.*, 2023, 147506.
26 H. Song, K. Zhang, P. Li, G. Qin, W. Xiao and C. Zhang, *et al.*, One-step construction of silver–polyaniline nanocomposite modified multifunctional sponges for wastewater remediation: adsorption, catalysis and antimicrobial applications, *J. Mater. Chem. A*, 2024, **12**, 6747–6767.
27 M. Hafeez, M. Faheem, Z. U. Abdin, K. Ahmad, S. Fazil and B. Khan, Synthesis and characterization of polyaniline-based conducting polymer and its anti-corrosion application, *Dig. J. Nanomater. Bios.*, 2017, **12**, 707–717.
28 F. Gao, J. Mu, Z. Bi, S. Wang and Z. Li, Recent advances of polyaniline composites in anticorrosive coatings: a review, *Prog. Org. Coat.*, 2021, **151**, 106071.
29 L. Liu, X.-B. Luo, L. Ding and S.-L. Luo, Application of nanotechnology in the removal of heavy metal from water, *Nanomaterials for the removal of pollutants and resource reutilization*, Elsevier, 2019, pp. 83–147.
30 X.-T. Yuan, L. Wu, H.-Z. Geng, L. Wang, W. Wang and X.-S. Yuan, *et al.*, Polyaniline/polysulfone ultrafiltration membranes with improved permeability and anti-fouling behavior, *J. Water Process Eng.*, 2021, **40**, 101903.
31 V. Goel, R. Tanwar, A. K. Saikia and U. K. Mandal, Separation Characteristics of Surface Modified Polysulfone Ultrafiltration Membrane using Oxidative Catalytic Polymerization of Aniline, *J. Polym. Mater.*, 2022, **39**, 283–305.
32 R. Erragued, M. Sharma, C. Costa, M. Bouaziz and L. M. Gando-Ferreira, Novel polyethersulfone mixed matrix adsorptive nanofiltration membrane fabricated from embedding zinc oxide coated by polyaniline, *J. Environ. Chem. Eng.*, 2023, **11**, 111607.
33 G. Song, H. Xu and L. Wang, Preparation and characterization of PSF porous composite nanofibers via solution-blowing as adsorbent for dye removal, *J. Polym. Res.*, 2023, **30**, 261.
34 X.-S. Yuan, Z.-Y. Guo, H.-Z. Geng, D. S. Rhen, L. Wang and X.-T. Yuan, *et al.*, Enhanced performance of conductive polysulfone/MWCNT/PANI ultrafiltration membrane in an online fouling monitoring application, *J. Membr. Sci.*, 2019, **575**, 160–169.
35 W. K. Maser, A. M. Benito, M. A. Callejas, T. Seeger, M. Martınez and J. Schreiber, *et al.*, Synthesis and characterization of new polyaniline/nanotube composites, *Mater. Sci. Eng., C*, 2003, **23**, 87–91.
36 X. Wu, Y. Wang, Y. Xiao, Y. Han, T. Li and Y. Ma, Synthesis and formation mechanism of PANI nanotubes prepared via facile aqueous solution polymerization, *Synth. Met.*, 2022, **291**, 117212.
37 F. Li, J. Li, L. Chen, Y. Dong, P. Xie and Q. Li, Preparation of CoB nanoparticles decorated PANI nanotubes as catalysts for hydrogen generation from $NaBH_4$ hydrolysis, *J. Taiwan Inst. Chem. Eng.*, 2021, **122**, 148–156.
38 K. Wetchakun, N. Wetchakun and S. Sakulsermsuk, An overview of solar/visible light-driven heterogeneous photocatalysis for water purification: TiO_2-and ZnO-based photocatalysts used in suspension photoreactors, *J. Ind. Eng. Chem.*, 2019, **71**, 19–49.
39 A. A. Barzinjy, Structure, synthesis and applications of ZnO nanoparticles: a review, *Jordan J. Phys.*, 2020, **13**, 123–135.
40 W. Y. Pang, A. L. Ahmad and N. D. Zaulkiflee, Antifouling and antibacterial evaluation of ZnO/MWCNT dual nanofiller polyethersulfone mixed matrix membrane, *J. Environ. Manage.*, 2019, **249**, 109358.
41 T. S. Vo, M. M. Hossain, H. M. Jeong and K. Kim, Heavy metal removal applications using adsorptive membranes, *Nano Converge.*, 2020, **7**, 36.
42 B. Zhao, X. Huang, X. Wu, L. Wang, A. Liu and Z. Zhang, *et al.*, Preparation of Fe_3O_4/polysulfone ultrafiltration membrane and its adsorption of phosphate from aqueous solution, *Desalin. Water Treat.*, 2018, **116**, 39–48.
43 M. Enfrin, J. Lee, P. Le-Clech and L. F. Dumée, Kinetic and mechanistic aspects of ultrafiltration membrane fouling by nano-and microplastics, *J. Membr. Sci.*, 2020, **601**, 117890.
44 D. Ponnamma, Y. Elgawady, M. K. Hassan, S. Adham, M. Al-Maas and K. Alamgir, *et al.*, Electrospun Polysulfone Hybrid Nanocomposite Fibers as Membrane for Separating Oil/Water Emulsion, *Water Conserv. Sci. Eng.*, 2023, **8**, 57.
45 D. J. Miller, D. R. Paul and B. D. Freeman, An improved method for surface modification of porous water purification membranes, *Polymer*, 2014, **55**, 1375–1383.
46 V. Vatanpour, M. Jouyandeh, H. Akhi, S. S. M. Khadem, M. R. Ganjali and H. Moradi, *et al.*, Hyperbranched polyethylenimine functionalized silica/polysulfone nanocomposite membranes for water purification, *Chemosphere*, 2022, **290**, 133363.
47 X. Zhang, J. Ma, J. Zheng, R. Dai, X. Wang and Z. Wang, Recent advances in nature-inspired antifouling membranes for water purification, *Chem. Eng. J.*, 2022, **432**, 134425.
48 V. Vatanpour, S. S. M. Khadem, A. Dehqan, S. Paziresh, M. R. Ganjali and M. Mehrpooya, *et al.*, Application of g-C_3N_4/ZnO nanocomposites for fabrication of anti-fouling polymer membranes with dye and protein rejection superiority, *J. Membr. Sci.*, 2022, **660**, 120893.
49 G. Moradi, S. Zinadini and L. Rajabi, Development of the tetrathioterephthalate filler incorporated PES nanofiltration membrane with efficient heavy metal ions rejection and superior antifouling properties, *J. Environ. Chem. Eng.*, 2020, **8**, 104431.
50 C. Latha, D. Lakshmi, P. Maheswari and D. Mohan, Preparation and performance of PU/Cpsf blend ultrafiltration membranes for removal of heavy metal ion rejection studies, *Eng. Technol. J.*, 2022, **40**, 1275–1283.

51 V. Nayak, M. Jyothi, R. G. Balakrishna, M. Padaki and A. M. Isloor, Synthesis and characterization of novel sulfanilic acid–polyvinyl chloride–polysulfone blend membranes for metal ion rejection, *RSC Adv.*, 2016, **6**, 25492–25502.

52 Y. Liu, J. Wang, Y. Wang, H. Zhu, X. Xu and T. Liu, *et al.*, High-flux robust PSf-*b*-PEG nanofiltration membrane for the precise separation of dyes and salts, *Chem. Eng. J.*, 2021, **405**, 127051.

53 H. Wu, H. Zhao, Y. Lin, X. Liu, H. Yao and L. Yu, *et al.*, Fabrication of polysulfone membrane with sponge-like structure by using different non-woven fabrics, *Sep. Purif. Technol.*, 2022, **297**, 121553.

54 L.-F. Liu, X.-L. Gu, X. Xie, R.-H. Li, C.-Y. Yu and X.-X. Song, *et al.*, Modification of PSf/SPSf blended porous support for improving the reverse osmosis performance of aromatic polyamide thin film composite membranes, *Polymers*, 2018, **10**, 686.

55 F. Gao, J. Wang, H. Zhang, H. Jia, Z. Cui and G. Yang, Aged PVDF and PSF ultrafiltration membranes restored by functional polydopamine for adjustable pore sizes and fouling control, *J. Membr. Sci.*, 2019, **570**, 156–167.

56 N. Li, W. Wang, C. Ma, L. Zhu, X. Chen and B. Zhang, *et al.*, A novel conductive rGO/ZnO/PSF membrane with superior water flux for electrocatalytic degradation of organic pollutants, *J. Membr. Sci.*, 2022, **641**, 119901.

57 N. Nasrollahi, V. Vatanpour, S. Aber and N. M. Mahmoodi, Preparation and characterization of a novel polyethersulfone (PES) ultrafiltration membrane modified with a CuO/ZnO nanocomposite to improve permeability and antifouling properties, *Sep. Purif. Technol.*, 2018, **192**, 369–382.

58 H. Nawaz, M. Umar, A. Ullah, H. Razzaq, K. M. Zia and X. Liu, Polyvinylidene fluoride nanocomposite super hydrophilic membrane integrated with Polyaniline-Graphene oxide nano fillers for treatment of textile effluents, *J. Hazard. Mater.*, 2021, **403**, 123587.

59 N. Hnatchuk, T. Pawale and X. Li, Asymmetric polymer materials: synthesis, structure, and performance, *Polymer*, 2022, **242**, 124607.

60 E. L. Subtil, J. Goncalves, H. G. Lemos, E. C. Venancio, J. C. Mierzwa and J. D. S. de Souza, *et al.*, Preparation and characterization of a new composite conductive polyethersulfone membrane using polyaniline (PANI) and reduced graphene oxide (rGO), *Chem. Eng. J.*, 2020, **390**, 124612.

61 N. P. Khumalo, G. D. Vilakati, S. D. Mhlanga, A. T. Kuvarega, B. B. Mamba and J. Li, *et al.*, Dual-functional ultrafiltration nano-enabled PSf/PVA membrane for the removal of Congo red dye, *J. Water Process Eng.*, 2019, **31**, 100878.

62 A. Sarihan, Development of high-permeable PSf/PANI-PAMPSA composite membranes with superior rejection performance, *Mater. Today Commun.*, 2020, **24**, 101104.

63 A. Tabasum, A. Siddique, H. Razzaq, H. H. Nawaz, S. Razzaque and S. Tahir, *et al.*, Integrated synergy: PSF/PANI/GO membranes for dual-action textile dye detoxification, *Mater. Adv.*, 2024, **5**, 4736–4752.

64 V. A. Mooss, F. Hamza, S. S. Zinjarde and A. A. Athawale, Polyurethane films modified with polyaniline-zinc oxide nanocomposites for biofouling mitigation, *Chem. Eng. J.*, 2019, **359**, 1400–1410.

65 N. Koutahzadeh, M. R. Esfahani and P. E. Arce, Sequential use of UV/H_2O_2—(PSF/TiO_2/MWCNT) mixed matrix membranes for dye removal in water purification: membrane permeation, fouling, rejection, and decolorization, *Environ. Eng. Sci.*, 2016, **33**, 430–440.

66 S. M. Sontakke and V. Awate, The effect of synthesis parameters on the conductivity of PSf/PANI and PSf/PPy composite membranes, *Can. J. Chem. Eng.*, 2018, **96**, 564–572.

67 A. S. Butt, A. A. Qaiser, N. Abid and U. Mahmood, Novel polyaniline–polyethersulfone nanofiltration membranes: effect of *in situ* polymerization time on structure and desalination performance, *RSC Adv.*, 2022, **12**, 33889–33898.

68 O. T. Mahlangu, G. Mamba and B. B. Mamba, A facile synthesis approach for GO-ZnO/PES ultrafiltration mixed matrix photocatalytic membranes for dye removal in water: leveraging the synergy between photocatalysis and membrane filtration, *J. Environ. Chem. Eng.*, 2023, **11**, 110065.

69 P. Pramila and N. Gopalakrishnan, Enhancement of antibacterial activity in nanofillers incorporated PSF/PVP membranes, *Mater. Res. Express*, 2018, **5**, 045306.

70 M. Purushothaman, A. Harikrishnan, P. S. Kumar, J. George, G. Rangasamy and V. K. Vaidyanathan, Enhancement of antifouling properties, metal ions and protein separation of poly(ether-ether-sulfone) ultrafiltration membranes by incorporation of poly ethylene glycol and n-ZnO, *Environ. Res.*, 2023, **216**, 114696.

71 B. Hudaib, V. Gomes, J. Shi, C. Zhou and Z. Liu, Poly(vinylidene fluoride)/polyaniline/MWCNT nanocomposite ultrafiltration membrane for natural organic matter removal, *Sep. Purif. Technol.*, 2018, **190**, 143–155.

72 A. Sarihan and E. Eren, Novel high performanced and fouling resistant PSf/ZnO membranes for water treatment, *Membr. Water Treat*, 2017, **8**, 563–574.

73 R. J. Gohari, F. Korminouri, W. Lau, A. Ismail, T. Matsuura and M. Chowdhury, *et al.*, A novel super-hydrophilic PSf/HAO nanocomposite ultrafiltration membrane for efficient separation of oil/water emulsion, *Sep. Purif. Technol.*, 2015, **150**, 13–20.

74 C. Lavanya and R. G. Balakrishna, Naturally derived polysaccharides-modified PSF membranes: a potency in enriching the antifouling nature of membranes, *Sep. Purif. Technol.*, 2020, **230**, 115887.

75 H. Wang, W. Wang, L. Wang, B. Zhao, Z. Zhang and X. Xia, *et al.*, Enhancement of hydrophilicity and the resistance for irreversible fouling of polysulfone (PSF) membrane immobilized with graphene oxide (GO) through chloromethylated and quaternized reaction, *Chem. Eng. J.*, 2018, **334**, 2068–2078.

76 P. Bhatia, P. Bansal and R. Chandra, Advancements in Metal Oxide/Polymer Nanocomposite Utilized as Photocatalysts for Wastewater Remediation, *Hybrid Composite Materials: Experimental and Theoretical Analysis*, Springer, 2024, pp. 215–236.

77 A. Chandrashekar, M. Hegde, J. A. Gopi, N. Prabhu, D. A. Gopakumar and J. J. George, *et al.*, Metal/Metal Oxide

Nanoparticles Modified Polymeric Composite Membranes for Water Treatment, *Nanomater. Air Water Purif.*, 2024, 347–371.

78 U. Hani, Comprehensive review of polymeric nanocomposite membranes application for water treatment, *Alexandria Eng. J.*, 2023, **72**, 307–321.

79 Q. Wang, W. Lin, S. Chou, P. Dai and X. Huang, Patterned membranes for improving hydrodynamic properties and mitigating membrane fouling in water treatment: a review, *Water Res.*, 2023, **236**, 119943.

80 M. Shakak, R. Rezaee, A. Maleki, A. Jafari, M. Safari and B. Shahmoradi, *et al.*, Synthesis and characterization of nanocomposite ultrafiltration membrane (PSF/PVP/SiO_2) and performance evaluation for the removal of amoxicillin from aqueous solutions, *Environ. Technol. Innovation*, 2020, **17**, 100529.

81 G. Moradi, M. Rahimi and S. Zinadini, Antifouling nanofiltration membrane via tetrathioterephthalate coating on aniline oligomers-grafted polyethersulfone for efficient dye and heavy metal ion removal, *J. Environ. Chem. Eng.*, 2021, **9**, 104717.

82 M. Alhoshan, J. Alam, A. K. Shukla and A. A. Hamid, Polyphenylsulfone membrane blended with polyaniline for nanofiltration promising for removing heavy metals (Cd^{2+}/Pb^{2+}) from wastewater, *J. Mater. Res. Technol.*, 2023, **24**, 6034–6047.

83 S. Mondal and S. K. Majumder, Fabrication of the polysulfone-based composite ultrafiltration membranes for the adsorptive removal of heavy metal ions from their contaminated aqueous solutions, *Chem. Eng. J.*, 2020, **401**, 126036.

84 S. Ahmadipouya, S. A. Mousavi, A. Shokrgozar and D. V. Mousavi, Improving dye removal and antifouling performance of polysulfone nanofiltration membranes by incorporation of UiO-66 metal-organic framework, *J. Environ. Chem. Eng.*, 2022, **10**, 107535.

85 Y. Liu, Q. Li, Y. Ji, M. Younas and B. He, Preparation of polyaniline conductive membranes through immersion of dopant solution for dye/salt separation, *Sep. Purif. Technol.*, 2024, **348**, 127531.

86 N. Baig, A. Matin, M. Faizan, D. Anand, I. Ahmad and S. A. Khan, Antifouling low-pressure highly permeable single step produced loose nanofiltration polysulfone membrane for efficient Erichrome Black T/divalent salts fractionation, *J. Environ. Chem. Eng.*, 2022, **10**, 108166.

87 G. Syed Ibrahim, A. M. Isloor, A. Ismail and R. Farnood, One-step synthesis of zwitterionic graphene oxide nanohybrid: application to polysulfone tight ultrafiltration hollow fiber membrane, *Sci. Rep.*, 2020, **10**, 6880.

88 A. Ahmadi, M. H. Sarrafzadeh, M. Mohamadi, Z. Mahdigholian and A. Hosseinian, Investigation on polysulfone blended NH_2-MIL125 (Ti) membrane for photocatalytic degradation of Methylene Blue dye, *J. Water Environ. Nanotechnol.*, 2020, **5**, 234–245.

89 M. M. Ayad and A. A. El-Nasr, Adsorption of Cationic Dye (Methylene Blue) from Water Using Polyaniline Nanotubes Base, *J. Phys. Chem. C*, 2010, **114**, 14377–14383.

90 F. Salehi-Babarsad, E. Derikvand, M. Razaz, R. Yousefi and A. Shirmardi, Heavy metal removal by using ZnO/organic and ZnO/inorganic nanocomposite heterostructures, *Int. J. Environ. Anal. Chem.*, 2020, **100**, 702–719.

91 A. M. Nasir, P. S. Goh, M. S. Abdullah, B. C. Ng and A. F. Ismail, Adsorptive nanocomposite membranes for heavy metal remediation: recent progresses and challenges, *Chemosphere*, 2019, **232**, 96–112.

92 L. Ahmadian-Alam and H. Mahdavi, A novel polysulfone-based ternary nanocomposite membrane consisting of metal–organic framework and silica nanoparticles: as proton exchange membrane for polymer electrolyte fuel cells, *Renewable Energy*, 2018, **126**, 630–639.

93 Y.-L. Lin, N.-Y. Zheng, Y.-J. Chen and C.-C. Chang, Incorporation of zeolitic imidazolate framework-8 (ZIF-8) in the polyamide and polysulfone layers of forward osmosis membranes for enhancing aquaculture wastewater recovery and PPCPs removal, *J. Water Process Eng.*, 2024, **66**, 105980.

94 M. K. Mohammed and M. Shekargoftar, Surface treatment of ZnO films with carbon nanotubes for efficient and stable perovskite solar cells, *Sustainable Energy Fuels*, 2021, **5**, 540–548.

95 T. D. Kusworo, F. Dalanta, N. Aryanti and N. H. Othman, Intensifying separation and antifouling performance of PSf membrane incorporated by GO and ZnO nanoparticles for petroleum refinery wastewater treatment, *J. Water Process Eng.*, 2021, **41**, 102030.

96 H. Alhweij, E. A. C. Emanuelsson, S. Shahid and J. Wenk, Simplified in-situ tailoring of cross-linked self-doped sulfonated polyaniline (S-PANI) membranes for nanofiltration applications, *J. Membr. Sci.*, 2021, **637**, 119654.

97 P. He, S. Zhao, C. Mao, Y. Wang, G. Ma and Z. Wang, *et al.*, *In situ* growth of double-layered polyaniline composite membrane for organic solvent nanofiltration, *Chem. Eng. J.*, 2021, **420**, 129338.

98 T. van den Berg and M. Ulbricht, Polymer nanocomposite ultrafiltration membranes: the influence of polymeric additive, dispersion quality and particle modification on the integration of zinc oxide nanoparticles into polyvinylidene difluoride membranes, *Membranes*, 2020, **10**, 197.

99 J. Li, M. Hu, H. Pei, X. Ma, F. Yan and D. S. Dlamini, *et al.*, Improved water permeability and structural stability in a polysulfone-grafted graphene oxide composite membrane used for dye separation, *J. Membr. Sci.*, 2020, **595**, 117547.

100 M. E. Khomri, N. E. Messaoudi, A. Dbik, S. Bentahar, Y. Fernine and A. Bouich, *et al.*, Modification of low-cost adsorbent prepared from agricultural solid waste for the adsorption and desorption of cationic dye, *Emergent Mater.*, 2022, **5**, 1679–1688.

101 B. Qiu, Q. Shao, J. Shi, C. Yang and H. Chu, Application of biochar for the adsorption of organic pollutants from wastewater: modification strategies, mechanisms and challenges, *Sep. Purif. Technol.*, 2022, **300**, 121925.

102 H. Sanaeepur, A. E. Amooghin, M. M. A. Shirazi, M. Pishnamazi and S. Shirazian, Water desalination and ion removal using mixed matrix electrospun nanofibrous membranes: a critical review, *Desalination*, 2022, **521**, 115350.

103 T. Ahmad, V. Pandey, M. S. Husain and S. Munjal, Structural and spectroscopic analysis of pure phase hexagonal wurtzite ZnO nanoparticles synthesized by sol–gel, *Mater. Today: Proc.*, 2022, **49**, 1694–1697.